



# Degeneration and Regeneration of Subbasal Corneal Nerves after Infectious Keratitis

## Citation

Müller, Rodrigo T., Farshad Abedi, Andrea Cruzat, Deborah Witkin, Neda Baniyasi, Bernardo M. Cavalcanti, Arsia Jamali, et al. 2015. "Degeneration and Regeneration of Subbasal Corneal Nerves after Infectious Keratitis." *Ophthalmology* 122 (11) (November): 2200–2209. doi:10.1016/j.optha.2015.06.047.

## Published Version

10.1016/j.optha.2015.06.047

## Permanent link

<http://nrs.harvard.edu/urn-3:HUL.InstRepos:34836849>

## Terms of Use

This article was downloaded from Harvard University's DASH repository, and is made available under the terms and conditions applicable to Open Access Policy Articles, as set forth at <http://nrs.harvard.edu/urn-3:HUL.InstRepos:dash.current.terms-of-use#OAP>

## Share Your Story

The Harvard community has made this article openly available.  
Please share how this access benefits you. [Submit a story](#).

[Accessibility](#)



# HHS Public Access

Author manuscript

*Ophthalmology*. Author manuscript; available in PMC 2016 November 01.

Published in final edited form as:

*Ophthalmology*. 2015 November ; 122(11): 2200–2209. doi:10.1016/j.ophtha.2015.06.047.

## Degeneration and Regeneration of Subbasal Corneal Nerves after Infectious Keratitis: A Longitudinal In Vivo Confocal Microscopy Study

Rodrigo Müller, MD<sup>1,2</sup>, Farshad Abedi, MD, DMedSc<sup>1,2</sup>, Andrea Cruzat, MD<sup>1,2</sup>, Deborah Witkin<sup>1,2</sup>, Neda Baniyasi<sup>1,2</sup>, Bernardo M. Cavalcanti, MD<sup>1,2</sup>, Arsia Jamali, MD<sup>1</sup>, James Chodosh, MD, MPH<sup>2</sup>, Reza Dana, MD<sup>2</sup>, Deborah Pavan-Langston, MD<sup>2</sup>, and Pedram Hamrah, MD<sup>1,2</sup>

<sup>1</sup>Ocular Surface Imaging Center, Massachusetts Eye & Ear Infirmary, Department of Ophthalmology, Harvard Medical School, 243 Charles Street, Boston, MA 02114, USA

<sup>2</sup>Cornea & Refractive Surgery Service, Massachusetts Eye & Ear Infirmary, Department of Ophthalmology, Harvard Medical School, 243 Charles Street, Boston, MA 02114, USA

### Abstract

**Purpose**—To investigate the longitudinal alterations of subbasal corneal nerves in patients with infectious keratitis (IK) during acute phase, cessation of treatment and recovery phase by *in vivo* confocal microscopy (IVCM).

**Design**—Prospective, longitudinal, case-control, single-center study.

**Subjects**—Fifty-six eyes of 56 patients with the diagnosis of bacterial (n=28), fungal (n=15), and *Acanthamoeba* (n=13) keratitis were included in the study. Thirty eyes of 30 normal volunteers constituted the control group.

**Methods**—Corneal sensation and serial IVCM of the central cornea were performed prospectively, by using the Heidelberg Retina Tomograph 3/Rostock Cornea Module (Heidelberg Engineering, Germany). IVCM images were assessed at 3 time points: at the first visit of the patient to the cornea service, at cessation of antimicrobial treatment, and up to six months after the resolution of infection.

**Main outcome measures**—Total nerve number and length, main nerve trunks, branching and corneal sensation were assessed during the follow-up period.

**Results**—Corneal nerves were significantly reduced during the acute phase in eyes with IK compared with controls across all subgroups, with total nerve length of  $5.47 \pm 0.69$  vs.  $20.59 \pm$

---

Reprint requests: Pedram Hamrah, M.D, Ocular Surface Imaging Center, Cornea and Refractive Surgery Service, Massachusetts Eye & Ear Infirmary, Harvard Medical School, 243 Charles Street, Boston, MA 02114, USA., pedram\_hamrah@meei.harvard.edu; p\_hamrah@yahoo.com Phone: 617-391-5865; Fax: 617-573-4300.

**Conflict of Interest:** The authors have no financial/conflicting interests to disclose.

**Publisher's Disclaimer:** This is a PDF file of an unedited manuscript that has been accepted for publication. As a service to our customers we are providing this early version of the manuscript. The manuscript will undergo copyediting, typesetting, and review of the resulting proof before it is published in its final citable form. Please note that during the production process errors may be discovered which could affect the content, and all legal disclaimers that apply to the journal pertain.

1.06 mm/mm<sup>2</sup>;  $p < 0.0001$ . At the cessation of treatment, corneal nerves in patients with IK had regenerated, including total nerve length ( $8.49 \pm 0.94$ ;  $p = 0.02$ ) and nerve branch length ( $4.80 \pm 0.37$ ;  $p = 0.005$ ). During the recovery phase, after resolution of infection, corneal nerves further regenerated, including total nerve length ( $12.13 \pm 1.97$ ;  $p = 0.005$ ), main nerve trunk length ( $5.80 \pm 1.00$ ;  $p = 0.01$ ) and nerve branch length ( $6.33 \pm 0.76$ ;  $p = 0.003$ ) as compared to the acute phase, but were still significantly lower when compared to controls ( $p < 0.05$  for all parameters). Corneal degeneration and regeneration correlated with corneal sensation ( $r = 0.47$ ,  $p = 0.0009$ ).

**Conclusion**—Patients with IK, suffering from profound loss of corneal nerves during the acute phase of infection, demonstrate an increase of corneal nerve density during the first six months after the resolution of infection. However, despite significant nerve regeneration, corneal nerve density does not fully recover and remains low as compared to controls. By providing an objective methodology to monitor corneal re-innervation, IVCM adds potentially important findings that may have implications for clinical management and surgical planning.

## INTRODUCTION

Infectious keratitis (IK) is a vision-threatening disease that varies in incidence depending upon geographic location and predisposing risk factors. It is estimated that 30,000 new cases of IK (including bacteria, fungus and *Acanthamoeba*) occur annually in the United States.<sup>1,2</sup> These microorganisms trigger an immune response, leading to severe corneal inflammation, ulceration and scarring.<sup>1,3–8</sup> The corneal ulceration and the subsequent scarring may result in corneal nerve damage with clinical consequences, due to impaired corneal nerve function.

The human cornea is supplied by the terminal branches of the ophthalmic division of the trigeminal nerve and is the most densely innervated tissue of the body.<sup>1,4,9–14</sup> Nerves penetrate the cornea in the deep peripheral stroma in a radial distribution and then course anteriorly, running parallel to the ocular surface, forming the subbasal nerve plexus between the Bowman's layer and the basal epithelium.<sup>1,8</sup> Corneal innervation has important trophic functions and plays an important role in the regulation of epithelial integrity, proliferation, and wound healing.<sup>1,3,6,8</sup> Although herpetic keratitis is the entity most frequently associated with a decrease in the subbasal corneal nerve plexus and with neurotrophic keratopathy, other infectious diseases may be associated with corneal nerve loss as well.<sup>4,9,11–14</sup>

Laser *in vivo* confocal microscopy (IVCM) is a non-invasive, high-resolution tool that allows imaging of the living cornea at the cellular level, providing images comparable with histochemical methods.<sup>8,9,11</sup> In recent years, the use of IVCM has revealed the importance of corneal nerves in both healthy eyes and ocular diseases, including infectious keratitis, cornea transplantations, laser keratorefractive surgeries, neurotrophic keratopathy and dry eye disease.<sup>4,15,16</sup> Using IVCM, we have recently demonstrated a decrease in corneal nerves and an increase in immune dendritic cells in patients with microbial keratitis.<sup>9,11</sup> While these findings may have significant clinical and surgical implications, no longitudinal studies have yet been performed in these patients to assess whether corneal nerve damage persists or resolves through re-innervation.

The aim of the present study was to investigate the longitudinal changes in subbasal corneal nerves in patients with *Acanthamoeba*, fungal and bacterial keratitis beyond the treatment

period. We hypothesized that corneal re-innervation takes place after the acute phase of infectious keratitis. Herein, we describe the level of nerve degeneration in the acute phase of infectious keratitis and regeneration after resolution of infection.

## METHODS

### Patients

This was a prospective, longitudinal, single-center study, conducted in a controlled, single-blinded fashion. Fifty-six eyes of 56 patients treated for acute infectious keratitis at the Cornea Service of the Massachusetts Eye & Ear Infirmary (MEEI), Boston, MA, USA between 2008 to 2014 were included in the study. Thirty eyes of 30 normal volunteers comprised the control group, out of which 18 were contact lens wearers. This study was Health Insurance Portability and Accountability Act (HIPAA)-compliant, adhered to the tenets of the Declaration of Helsinki, and was approved by the Institutional Review Board (IRB)/Ethics Committee of our institution. Written informed consent was obtained from all subjects after a detailed explanation of the nature of the study.

The diagnosis of acute infectious keratitis was made by cornea specialists based on clinical history and ophthalmic examination. All patients and healthy controls underwent slit-lamp bio-microscopy. Only patients with positive corneal cultures or positive confocal findings for fungal or *Acanthamoeba* keratitis were included. The study excluded subjects with a history of any prior episode of infectious keratitis, ocular inflammatory disease, ocular trauma, previous eye surgery, and diabetes.

### *In Vivo* Confocal Microscopy

Laser scanning *in vivo* confocal microscopy (Heidelberg Retina Tomograph 3 with the Rostock Cornea Module, Heidelberg Engineering GmbH, Heidelberg, Germany) of the central cornea was performed in all subjects. This microscope uses a 670-nm red wavelength diode laser source, and it is equipped with a 63X objective immersion lens with a numerical aperture of 0.9 (Olympus, Tokyo, Japan). The IVCM provides images that represent a coronal section of the cornea of 400 X 400  $\mu\text{m}$ , which is 160,000  $\mu\text{m}^2$ , at a selectable corneal depth and is separated from adjacent images by approximately 1 to 4  $\mu\text{m}$  and lateral resolution of 1  $\mu\text{m}/\text{pixel}$ .

Digital images were stored on a computer workstation at 30 frames/per second. A disposable sterile polymethylmethacrylate cap (Tomo-Cap; Heidelberg Engineering GmbH, Heidelberg, Germany), filled with a layer of hydroxypropyl methylcellulose 2.5% (Genteal gel, Novartis Ophthalmics) in the bottom, was mounted in front of the Rostock Cornea Module optics for each examination. One drop of topical anesthesia of 0.5% proparacaine hydrochloride (Alcaine, Alcon) was instilled in both eyes, followed by a drop of hydroxypropyl methylcellulose 2.5% (GenTeal gel, Novartis Ophthalmics) in both eyes. One drop of hydroxypropyl methylcellulose 2.5% was also placed on the outside tip of the Tomo-Cap to improve optical coupling, and manually advanced until the gel contacted the central surface of the cornea.

IVCM was performed at three time points for each study eye: at the first visit of the patient to the cornea service (acute phase), at the day of cessation of antimicrobial treatment, and also at their last visit in the interval between one to six months after cessation of antimicrobial treatment (recovery phase). A total of six to eight volume and sequence scans per time point were obtained from the center of each cornea, at least three of which were sequence scans with particular focus on the subepithelial area and the subbasal nerve plexus, typically at a depth of 50 to 80  $\mu\text{m}$ . Sequence scans allow imaging the same area continuously, permitting the capture of large numbers of images of the subbasal nerve plexus per scan. Thus, the scans yielded 300–400 images of the subbasal layer alone. When a corneal ulcer was present with an epithelial defect, both the ulcer and the surrounding areas were scanned.

### Corneal Sensation

Corneal sensation was measured in the central area of the cornea with the Cochet-Bonnet esthesiometer (Luneau Ophthalmologie, Chartres, France) in all subjects as previously described.<sup>13</sup> This test mechanically stimulates corneal nerves by touching the tip of a retractable 6.0-cm long monofilament nylon thread of 0.12-mm diameter against the corneal surface, decreasing in steps of 1.0 cm if a positive response was not obtained or advancing by 0.5 cm if a positive response was obtained. The longest filament length that resulted in a positive response was considered the corneal threshold.

### Data Analysis

Three representative images were selected for analysis of each eye for each time point. The images were selected from the layer immediately at or posterior to the basal epithelial layer and anterior to the Bowman's layer by one experienced observer (R.M.). The criteria for selecting the images were the best-focused and most complete images, with the whole image in the same layer, without motion, without folds and with good contrast. Two observers (R.M. and F.A.), masked to the study groups and diagnoses, performed the IVCM image analyses. The nerve analysis was done using the semi-automated tracing program NeuronJ,<sup>17–19</sup> a plug-in for ImageJ (<http://www.image-science.org/meijering/software>). Nerve density was assessed by measuring the total length of the nerve fibers in micrometers. Main nerve trunk was defined as the total number of main nerve trunks in one image after analyzing the images anterior and posterior to the analyzed image in order to confirm that these did not branch from other nerves. Nerve branching was defined as the total number of nerve branches in one image. The number of total nerves measured was defined as the number of all nerves, including main nerve trunks and branches in one image (Fig. 1).

### Statistical Analysis

Statistical analysis was performed using Stata version 13.0 (Stata Corp, TX, USA). Continuous variables were expressed as mean  $\pm$  standard error of the mean, whereas categorical variables were described by frequency and percentage, unless otherwise indicated. The distribution of data was investigated using Shapiro-Wilk normality test. Chi-square test was applied to compare qualitative variables. Wilcoxon signed-rank test (for paired groups) or Kruskal-Wallis (for unpaired groups) were used to assess differences between visits or groups. Bonferroni post-hoc test was used for further analysis, when

appropriate. Spearman's correlation coefficient was used to determine the correlation of nerve changes from baseline (acute phase) and the time of the two follow-up visits. Multiple linear regression was applied to assess predictors of nerve parameters, using age, gender, contact lens use and time of the follow-up visits as independent variables. For each test, a p-value of less than 0.05 was considered significant.

## RESULTS

Fifty-six eyes of 56 patients (31 male and 25 female) with *Acanthamoeba* (n=13), fungal (n=15) or bacterial (n=28) keratitis met the inclusion and exclusion criteria, were recruited, and constituted the infectious keratitis (IK) group. Thirty healthy eyes of 30 volunteers (10 male and 20 female) comprised the control group, matched for age and contact lens use. Figure 2 shows representative slit-lamp photographs and IVCM images of the study groups. The mean age was  $42.4 \pm 2.1$  and  $42.3 \pm 2.1$  years in patients and controls, respectively ( $p=0.47$ ). Patients with *Acanthamoeba*, fungal and bacterial keratitis were treated with topical antimicrobials for an average of  $366.8 \pm 73.4$ ,  $135.4 \pm 31.8$  and  $35.3 \pm 5.7$  days, respectively. Table 1 presents the demographics and treatment duration of these groups.

### Subbasal Corneal Nerve Alterations by IVCM

**Nerve Alterations During the Acute Phase**—The total subbasal nerve length during the acute phase was  $5.47 \pm 0.69$  mm/mm<sup>2</sup> for the combined IK group and was  $2.91 \pm 0.64$ ,  $4.65 \pm 0.95$ , and  $7.71 \pm 1.24$  mm/mm<sup>2</sup> for the *Acanthamoeba*, fungal, and bacterial keratitis groups, respectively ( $p<0.0001$  for all, compared to controls:  $21.59 \pm 1.06$  mm/mm<sup>2</sup>). A significant diminishment in the main nerve trunk length ( $2.44 \pm 0.42$  mm/mm<sup>2</sup>) and in the nerve branch length ( $3.03 \pm 0.24$  mm/mm<sup>2</sup>) was found in the combined IK group as compared to controls ( $10.61 \pm 0.46$  and  $10.98 \pm 0.80$  mm/mm<sup>2</sup>, respectively) and also in the *Acanthamoeba*, fungal and bacterial subgroups ( $p<0.0001$  for all).

The total number of subbasal nerves during the acute phase was decreased in the combined IK group ( $3.70 \pm 0.35$  nerves/frame) and also in the *Acanthamoeba* ( $2.36 \pm 0.40$ ), fungal ( $3.27 \pm 0.53$ ) and bacterial ( $4.66 \pm 0.65$ ) subgroups, as compared to controls ( $20.00 \pm 1.80$ ,  $p<0.0001$  for all). Moreover, a significant diminishment in the number of main nerve trunks and nerve branches was found in the combined IK group, as well as in all the subgroups, as compared to controls ( $p<0.0001$  for all, Tables 2 and 3).

**Nerve Alterations During Cessation of Treatment Phase**—The total subbasal nerve length during the cessation of treatment showed a significant increase compared to the acute phase in the combined IK group ( $8.49 \pm 0.94$  vs.  $5.47 \pm 0.69$  mm/mm<sup>2</sup>,  $p=0.02$ ) and also in the *Acanthamoeba* subgroup ( $9.24 \pm 1.97$  vs.  $2.91 \pm 0.64$ ,  $p=0.01$ ); however, no statistical difference was found in the fungal ( $6.37 \pm 2.00$  vs.  $4.65 \pm 0.95$ ,  $p=0.89$ ) and bacterial subgroups ( $9.18 \pm 1.81$  vs.  $7.71 \pm 1.24$ ,  $p=0.18$ ). A significant increase in nerve branch length was found at the cessation of treatment compared to the acute phase, in the combined IK group ( $3.03 \pm 0.24$  vs.  $4.80 \pm 0.37$ ,  $p=0.005$ ). However, all the subgroups showed an increase in nerve branch length compared to the acute phase, although this was not statistically significant. The main nerve trunk length showed a slight increase in the combined IK group ( $3.69 \pm 0.64$  vs.  $2.44 \pm 0.42$  mm/mm<sup>2</sup>,  $p=0.13$ ); however, only in the

*Acanthamoeba* subgroup was this increase statistically significant ( $5.09 \pm 1.51$  vs.  $0.37 \pm 0.24$ ,  $p=0.01$ ). Figure 3 shows subbasal corneal nerve length alterations in the IK groups and controls over time.

A significant difference was found when comparing the total number of nerves during the cessation of treatment phase with the acute phase, including the combined IK group ( $5.50 \pm 0.55$  vs.  $3.70 \pm 0.35$  nerves/frame,  $p=0.009$ ) and the *Acanthamoeba* ( $5.91 \pm 0.87$  vs.  $2.36 \pm 0.40$ ,  $p=0.007$ ). Despite increasing on average, the fungal ( $4.38 \pm 1.16$  vs.  $3.27 \pm 0.53$ ,  $p=0.8$ ) and bacterial ( $5.85 \pm 1.02$  vs.  $4.66 \pm 0.65$ ,  $p=0.09$ ) subgroups did not showed significant differences. A significant increase in the number of nerve branches was found in the combined IK group, despite no difference observed in the number of main nerve trunks. The *Acanthamoeba* subgroup showed a significant increase in the number of main nerve trunks and nerve branches, whereas no difference was found in the fungal and in the bacterial subgroups (Table 3).

**Nerve Alterations During the Recovery Phase**—The total nerve length during the recovery phase showed a significant increase compared to the acute phase, in the combined IK group ( $12.13 \pm 1.97$  vs.  $5.47 \pm 0.69$  mm/mm<sup>2</sup>,  $p=0.005$ ) and also in the *Acanthamoeba* ( $12.70 \pm 2.77$  vs.  $2.91 \pm 0.64$  mm/mm<sup>2</sup>,  $p=0.04$ ) and fungal ( $14.85 \pm 3.12$  and  $4.65 \pm 0.95$ ,  $p=0.03$ ) subgroups. Furthermore, the main nerve trunk length and the nerve branch length showed an increase in the combined IK group, as well as in the *Acanthamoeba* and fungal subgroups. However, no statistical difference was found in the bacterial subgroup, when comparing the recovery phase to the acute phase, regarding the total nerve length, main nerve trunk length and nerve branch length (Table 3).

The total number of nerves during the recovery phase (Figure 4) showed a significant increase, compared to the acute phase in the combined IK group ( $7.85 \pm 1.16$  vs.  $3.70 \pm 0.35$  nerves/frame,  $p=0.007$ ) as well as in the *Acanthamoeba* ( $8.12 \pm 1.77$  vs.  $2.36 \pm 0.40$ ,  $p=0.04$ ) and fungal subgroups ( $9.82 \pm 2.26$  vs.  $3.27 \pm 0.53$ ,  $p=0.03$ ).

Despite the nerve regeneration over time, the total nerve length and number of total nerves were still significantly lower compared to controls in the combined IK group ( $12.13 \pm 1.97$  mm/mm<sup>2</sup>,  $p=0.002$  and  $7.85 \pm 1.16$  nerves/frame, respectively,  $p<0.0001$ ), in the *Acanthamoeba* ( $12.70 \pm 2.77$  mm/mm<sup>2</sup>,  $p=0.04$  and  $8.12 \pm 1.77$  nerves/frame,  $p=0.03$ ) and bacterial subgroups ( $9.39 \pm 3.28$  mm/mm<sup>2</sup>,  $p=0.002$  and  $5.99 \pm 2.16$  nerves/frame,  $p=0.01$ ).

**Corneal Nerve Regeneration:** Due to the variability of follow-up times among infectious keratitis subgroups, we investigated the correlation of nerve changes from baseline (acute phase) to the time of both follow-up visits. Figure 5 demonstrates the scatter plot of morphological nerve alterations over time. Total nerve length and the total nerve number increased significantly over time ( $R=0.46$ ,  $P=0.003$  and  $R=0.41$ ,  $p=0.01$ , respectively). After multiple adjustments for age, gender, and contact lens use, the association between the time of follow-up visits and the nerve density parameters, including total nerve length and total nerve number, remained significant in the linear regression model ( $p=0.009$  and  $0.03$ , respectively). The average rate of nerve regeneration was  $1.02 \pm 0.52$  mm/mm<sup>2</sup> per month in the combined IK group. While the rate of nerve regeneration, between the acute phase and

the cessation of treatment phase was  $0.61 \pm 0.15$  mm/mm<sup>2</sup> per month, the rate between the cessation of treatment phase and the recovery phase was  $1.60 \pm 0.56$  mm/mm<sup>2</sup> per month in the combined group. Moreover, the corneal sensation also increased over time, from  $3.9 \pm 0.4$  cm at the acute phase, to  $5.6 \pm 0.1$  cm at cessation of treatment and finally to  $5.9 \pm 0.1$  at the recovery phase ( $p=0.004$ ). The corneal sensation showed a significant correlation with total nerve length ( $r=0.47$ ,  $p=0.0009$ ), and total number of nerves ( $r=0.43$ ,  $p=0.002$ ).

## DISCUSSION

This prospective, longitudinal, controlled study demonstrates corneal nerve regeneration of the subbasal layer after resolution of infectious keratitis. We show that while corneal nerves do regenerate, they do not reach normal levels, even in the recovery phase, up to six months after cessation of treatment. To our knowledge, this is the first study that systematically analyzes changes in the corneal subbasal nerve plexus in patients with IK, beyond the acute phase of infection. We have previously demonstrated a decrease in the subbasal corneal nerve density during the acute phase of IK, including *Acanthamoeba*, fungal and bacterial keratitis.<sup>9,11</sup>

*In vivo* confocal microscopy has routinely been used for diagnostic purposes in patients with *Acanthamoeba* and fungal keratitis over the past several years.<sup>7,20,21</sup> More recently, attention to other histological cellular and structural details of the cornea, in particular the corneal nerve fibers, has yielded additional information regarding the status and prognosis of corneal health.<sup>4,11,15,22,23</sup> Until recently, the assessment of corneal innervation in the clinical setting has only been possible through the measurement of corneal sensation (e.g., by the Cochet-Bonnet esthesiometer or the Belmonte esthesiometer).<sup>17,19,24</sup> IVCN, and more recently laser IVCN, now allow for systematic studies of subbasal corneal nerve parameters in patients. Advantages of this device include its speed, ease of use, objectivity, and the non-invasiveness of the imaging procedure. Moreover, it allows for serial studies in patients providing histological features, a unique feature that is not possible with tissue biopsies.

Although corneal nerves regenerate during follow-up after resolution of the infection and cessation of treatment in the combined IK group, the IK subgroups do not show the same level of regeneration. The *Acanthamoeba* and fungal keratitis subgroups reveal an increase in subbasal nerve parameters at the recovery phase compared to the acute phase. However, this regeneration pattern is not noted in the bacterial subgroup. This can be explained by the fact that treatment duration and subsequent follow-up time for bacterial keratitis patients are much shorter, and thus the shorter follow-up time does not allow for detection of corneal nerves changes, which typically takes longer without active intervention.

The pharmacotherapy for IK is usually prolonged and toxic, particularly in cases of *Acanthamoeba* and fungal keratitis. Therefore, amoebicidal medication can result in corneal cytotoxicity. Dose- and time-dependent keratocyte cell death has previously been observed using polyhexamethylene biguanide and chlorhexidine.<sup>11,20</sup> Further, toxic keratopathy caused by propamidine has been described.<sup>11,22,25</sup> Berry et al. showed that with increased exposure to antibiotics, antifungals or their combinations, drug-dependent toxicity increases.



However, the toxicity of drug combinations is not merely cumulative; thus, decreasing the dose does not necessarily diminish the cytopathic effects.<sup>24,26</sup> Therefore it is conceivable that the prolonged and concurrent use, and the numerous combinations of antimicrobial eye drops used by patients with IK may be a limiting factor in the corneal re-innervation process.

The *Acanthamoeba* subgroup shows a reduction in the subbasal nerve density, which is more pronounced than the fungal and bacterial subgroups during the acute phase. This difference can be caused by the occurrence of perineuritis, a hallmark of *Acanthamoeba* keratitis. In addition, Pettit et al. showed that *Acanthamoeba* trophozoites were able to destroy nerve cells *in vitro*, both by cytolysis and by digestion.<sup>15,25,27–29</sup> A similar pattern of subbasal nerve damage during the acute phase of IK was previously addressed in a paper published by our group.<sup>11,30</sup>

In a recent cross-sectional study, Cruzat et al. demonstrated a strong and significant correlation between the increase in dendritiform cell density and the decrease in subbasal corneal nerves in patients with IK, suggesting a connection between corneal immune response and nerve alterations.<sup>11,15,31–33</sup> However, it is unknown whether the nerve damage observed during the acute phase is caused by severe corneal inflammation alone or may be related to pathogen-induced damage.<sup>11,25,27</sup> The resulting neurogenic inflammation is an important defense mechanisms that protects tissues from damage from a variety of pathogens, which can be a double-edged sword.<sup>34</sup> The exposure of the cornea to a microbial insult triggers the release of inflammatory cells and pro-inflammatory mediators. On the one hand, the production of pro-inflammatory cytokines results in the release of bioactive substances such as proteases, leading to extensive tissue injury.<sup>11,26</sup> On the other hand, it has been shown that neurotrophic factors (e.g., nerve growth factor and vascular endothelial growth factor) and inflammatory mediators (e.g., T lymphocytes and interleukins) are involved in immunomodulation, corneal nerve repair and regeneration.<sup>15,31–33,35</sup>

Previously, IVCN has also been used to assess re-innervation of the subbasal corneal nerves in patients subjected to surgical corneal procedures, such as photorefractive keratectomy (PRK), laser-assisted in-situ keratomileusis (LASIK), and corneal transplantation. In patients after PRK, subbasal nerves regenerate to near preoperative density within three years.<sup>15,28,29,36</sup> During LASIK procedures, stromal nerves are being transected at a much deeper layer than in advanced surface ablation procedures, with a decrease in the subbasal nerves of more than 80%, and a gradual but incomplete postoperative regeneration at two years.<sup>28,36,37</sup> In contrast, following corneal transplantation, subbasal and epithelial re-innervation of the donor graft occurs partially, although stromal innervation is limited. The subbasal nerve density may not recover to normal levels even after 40 years, with persistent anatomic disorganization of corneal nerves.<sup>38,39</sup> We observed a decrease in the subbasal nerve density during the acute phase of about 70%, compared to controls. Previous studies have demonstrated that the subbasal nerve regeneration rate post PRK and LASIK is approximately 25% and 33% at 6 months from the baseline, respectively.<sup>15</sup> During the recovery phase (from the cessation of the antimicrobial treatment to up six months thereafter), our study showed an increase of approximately 40% in the nerve density. Specifically, we show a regeneration rate between the acute phase and the cessation of the

antimicrobial treatment of  $0.61 \pm 0.15$  mm/mm<sup>2</sup> per month, whereas between the cessation of treatment and the recovery phase the regeneration rate almost triples, reaching  $1.60 \pm 0.56$  mm/mm<sup>2</sup> per month. Thus, regeneration of corneal nerves beyond the acute phase of the disease may be an important consideration in predicting the long-term prognosis of corneal health.

Lagali et al. reported that the subbasal nerve regeneration is delayed up to ten months after total Bowman's layer (BL) removal by phototherapeutic keratectomy (PTK). In addition, they showed that patients without BL had a delay in nerve regeneration compared to patients with partial BL, evidence that the partial preservation of the BL may promote faster regeneration of central subbasal nerves.<sup>37</sup> The impairment of the BL, presents in the majority of patients with corneal ulcers and IK, resulting in residual stromal scarring and fibrotic tissue, may be a possible factor that slows down or affects the re-innervation of the subbasal corneal nerves in these patients.

The correlation between corneal innervation and corneal sensation has previously been demonstrated in several studies.<sup>13,40,41</sup> In addition to their important sensory function, corneal nerves play a role in maintaining the functional integrity of the ocular surface by releasing neuronal factors that promote corneal epithelial homeostasis.<sup>42</sup> Diminished sensitivity due to impaired innervation may affect the afferent reflex arm, reducing tear production, blink reflex, avoidance of mechanical or chemical stimuli, and slowing the healing response by compromising the epithelium.<sup>42-44</sup> Moreover, a stable tear film, combined with a healthy corneal epithelium, provides a physical barrier against microbial invasion and environmental trauma.<sup>45,46</sup> Thus, the damage to corneal nerves may result in signs and symptoms of ocular surface disease, such as epithelial defects, superficial cornea vascularization, burning, foreign body sensation and light sensitivity.<sup>14</sup>

Long-term contact lens wear has been associated with a considerable reduction in corneal sensation.<sup>47-49</sup> Decreased oxygen and carbon dioxide gaseous exchange, leading to reductions in the pH of the cornea and consequently depressing nerve function, are potential factors affecting the corneal sensitivity.<sup>47</sup> However, while corneal nerve function has been shown to be altered, our study demonstrates that the corneal subbasal nerve density does not seem to be affected in our control contact lens users.<sup>48,49</sup> Moreover, regression analysis demonstrated that a positive history of contact lens wear did not show a significant effect on the rate of nerve regeneration in patients with IK.

A limitation of the present study is the fact that only the subbasal nerve plexus of the central cornea was analyzed; therefore, we cannot necessarily extrapolate our findings to the peripheral cornea. Moreover, poor topographic reproducibility and the difficulty of ensuring that the exact same locations are tested in all patients and at all time points are currently not optimal.

In conclusion, patients with IK reveal corneal nerve regeneration of subbasal nerves during the first six months after the resolution of infection and cessation of treatment. Nevertheless, the nerve density remains significantly lower than in the control group and thus did not reach normal levels. These findings may explain the development of ocular surface disease

after microbial keratitis,<sup>14,50–52</sup> suggesting that treatments promoting corneal re-innervation may prevent ocular surface disease in these patients. Future studies may elucidate the underlying mechanisms of corneal re-innervation in patients with infectious keratitis, allowing the development of therapeutic approaches.

## Acknowledgments

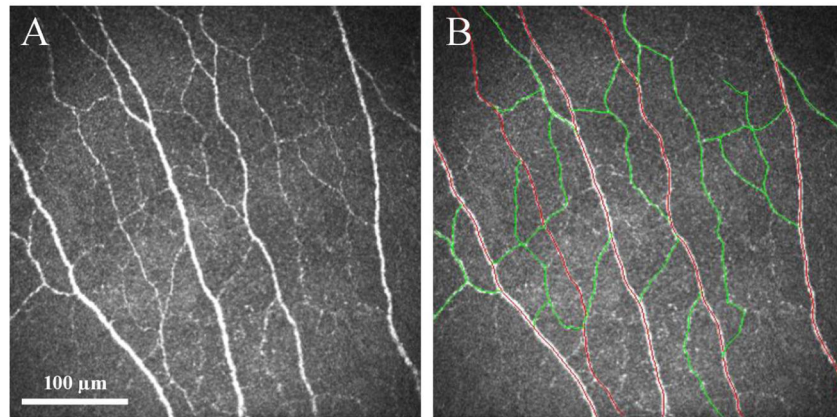
Financial Support: NIH K08-EY020575 (PH), Research to Prevent Blindness Career Development Award (PH), Research to Prevent Blindness Senior Scientific Investigator Award (JC), Falk Medical Research Trust (PH, JC), MEEI Foundation (PH). The funding organizations had no role in the design or conduct of this research.

## References

1. Müller LJ, Marfurt CF, Kruse F, Tervo TMT. Corneal nerves: structure, contents and function. *Exp Eye Res.* 2003; 76:521–542. [PubMed: 12697417]
2. Pepose JS, Wilhelmus KR. Divergent approaches to the management of corneal ulcers. *Am J Ophthalmol.* 1992; 114:630–632. [PubMed: 1443028]
3. Stern ME, Beuerman RW, Fox RI, et al. The pathology of dry eye: the interaction between the ocular surface and lacrimal glands. *Cornea.* 1998; 17:584–589. [PubMed: 9820935]
4. Cruzat A, Pavan-Langston D, Hamrah P. In vivo confocal microscopy of corneal nerves: analysis and clinical correlation. *Semin Ophthalmol.* 2010; 25:171–177. [PubMed: 21090996]
5. Mantopoulos D, Cruzat A, Hamrah P. In vivo imaging of corneal inflammation: new tools for clinical practice and research. *Semin Ophthalmol.* 2010; 25:178–185. [PubMed: 21090997]
6. Nishida T. Neurotrophic mediators and corneal wound healing. *Ocul Surf.* 2005; 3:194–202. [PubMed: 17131028]
7. Kumar RL, Cruzat A, Hamrah P. Current state of in vivo confocal microscopy in management of microbial keratitis. *Semin Ophthalmol.* 2010; 25:166–170. [PubMed: 21090995]
8. Oliveira-Soto L, Efron N. Morphology of corneal nerves using confocal microscopy. *Cornea.* 2001; 20:374–384. [PubMed: 11333324]
9. Kurbanyan K, Hoesl LM, Schrems WA, Hamrah P. Corneal nerve alterations in acute Acanthamoeba and fungal keratitis: an in vivo confocal microscopy study. *Eye (Lond).* 2012; 26:126–132. [PubMed: 22079969]
10. Müller LJ, Pels L, Vrensen GF. Ultrastructural organization of human corneal nerves. *Invest Ophthalmol Vis Sci.* 1996; 37:476–488. [PubMed: 8595948]
11. Cruzat A, Witkin D, Baniyadi N, et al. Inflammation and the nervous system: the connection in the cornea in patients with infectious keratitis. *Invest Ophthalmol Vis Sci.* 2011; 52:5136–5143. [PubMed: 21460259]
12. Hamrah P, Cruzat A, Dastjerdi MH, et al. Unilateral herpes zoster ophthalmicus results in bilateral corneal nerve alteration: an in vivo confocal microscopy study. *Ophthalmology.* 2013; 120:40–47. [PubMed: 22999636]
13. Hamrah P, Cruzat A, Dastjerdi MH, et al. Corneal sensation and subbasal nerve alterations in patients with herpes simplex keratitis: an in vivo confocal microscopy study. *Ophthalmology.* 2010; 117:1930–1936. [PubMed: 20810171]
14. Bonini S, Rama P, Olzi D, Lambiase A. Neurotrophic keratitis. *Eye (Lond).* 2003; 17:989–995. [PubMed: 14631406]
15. Shaheen BS, Bakir M, Jain S. Corneal nerves in health and disease. *Survey of Ophthalmology.* 2014; 59:263–285. [PubMed: 24461367]
16. Niederer RL, McGhee CNJ. Clinical in vivo confocal microscopy of the human cornea in health and disease. *Prog Retin Eye Res.* 2010; 29:30–58. [PubMed: 19944182]
17. Cochet P, Bonnet R. Corneal esthesiometry. Performance and practical importance. *Bull Soc Ophthalmol Fr.* 1961; 6:541–550. [PubMed: 13880071]

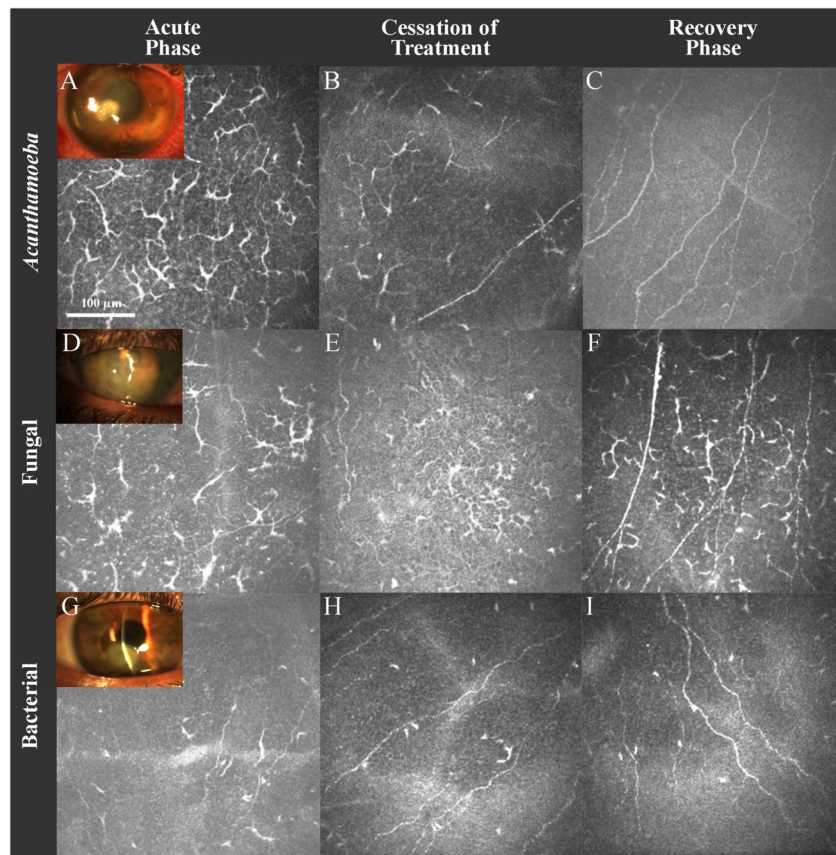
18. Meijering E, Jacob M, Sarria J-CF, et al. Design and validation of a tool for neurite tracing and analysis in fluorescence microscopy images. *Cytometry A*. 2004; 58:167–176. [PubMed: 15057970]
19. Belmonte C, Acosta MC, Schmelz M, Gallar J. Measurement of corneal sensitivity to mechanical and chemical stimulation with a CO2 esthesiometer. *Invest Ophthalmol Vis Sci*. 1999; 40:513–519. [PubMed: 9950612]
20. Lee J-E, Oum BS, Choi HY, et al. Cysticidal effect on acanthamoeba and toxicity on human keratocytes by polyhexamethylene biguanide and chlorhexidine. *Cornea*. 2007; 26:736–741. [PubMed: 17592327]
21. Chew SJ, Beuerman RW, Assouline M, et al. Early diagnosis of infectious keratitis with in vivo real time confocal microscopy. *CLAO J*. 1992; 18:197–201. [PubMed: 1499129]
22. Johns KJ, Head WS, O'Day DM. Corneal toxicity of propanidine. *Arch Ophthalmol*. 1988; 106:68–69. [PubMed: 3337709]
23. Villani E, Baudouin C, Efron N, et al. In vivo confocal microscopy of the ocular surface: from bench to bedside. *Curr Eye Res*. 2014; 39:213–231. [PubMed: 24215436]
24. Berry M, Gurung A, Easty DL. Toxicity of antibiotics and antifungals on cultured human corneal cells: effect of mixing, exposure and concentration. *Eye (Lond)*. 1995; 9 ( Pt 1):110–115. [PubMed: 7713237]
25. Pettit DA, Williamson J, Cabral GA, Marciano-Cabral F. In vitro destruction of nerve cell cultures by *Acanthamoeba* spp. : a transmission and scanning electron microscopy study. *J Parasitol*. 1996; 82:769–777. [PubMed: 8885887]
26. Dovi JV, Szpaderska AM, DiPietro LA. Neutrophil function in the healing wound: adding insult to injury? *Thromb Haemost*. 2004; 92:275–280. [PubMed: 15269822]
27. Pfister DR, Cameron JD, Krachmer JH, Holland EJ. Confocal microscopy findings of *Acanthamoeba* keratitis. *Am J Ophthalmol*. 1996; 121:119–128. [PubMed: 8623881]
28. Erie JC, McLaren JW, Hodge DO, Bourne WM. Recovery of corneal subbasal nerve density after PRK and LASIK. *Am J Ophthalmol*. 2005; 140:1059–1064. [PubMed: 16376651]
29. Patel DV, McGhee CNJ. In vivo confocal microscopy of human corneal nerves in health, in ocular and systemic disease, and following corneal surgery: a review. *Br J Ophthalmol*. 2009; 93:853–860. [PubMed: 19019923]
30. Darwish T, Brahma A, O'Donnell C, Efron N. Subbasal nerve fiber regeneration after LASIK and LASEK assessed by noncontact esthesiometry and in vivo confocal microscopy: prospective study. *J Cataract Refract Surg*. 2007; 33:1515–1521. [PubMed: 17720064]
31. Cohen A, Bray GM, Aguayo AJ. Neurotrophin-4/5 (NT-4/5) increases adult rat retinal ganglion cell survival and neurite outgrowth in vitro. *J Neurobiol*. 1994; 25:953–959. [PubMed: 7964706]
32. Li Z, Burns AR, Han L, et al. IL-17 and VEGF are necessary for efficient corneal nerve regeneration. *Am J Pathol*. 2011; 178:1106–1116. [PubMed: 21356362]
33. Zhong J, Dietzel ID, Wahle P, et al. Sensory impairments and delayed regeneration of sensory axons in interleukin-6-deficient mice. *J Neurosci*. 1999; 19:4305–4313. [PubMed: 10341234]
34. Beuerman RW, Stern ME. Neurogenic inflammation: a first line of defense for the ocular surface. *Ocul Surf*. 2005; 3:S203–6. [PubMed: 17216120]
35. Lambiase A, Rama P, Bonini S, et al. Topical treatment with nerve growth factor for corneal neurotrophic ulcers. *N Engl J Med*. 1998; 338:1174–1180. [PubMed: 9554857]
36. Moilanen JAO, Holopainen JM, Vesaluoma MH, Tervo TMT. Corneal recovery after lasik for high myopia: a 2-year prospective confocal microscopic study. *Br J Ophthalmol*. 2008; 92:1397–1402. [PubMed: 18650214]
37. Lagali N, Germundsson J, Fagerholm P. The role of Bowman's layer in corneal regeneration after phototherapeutic keratectomy: a prospective study using in vivo confocal microscopy. *Invest Ophthalmol Vis Sci*. 2009; 50:4192–4198. [PubMed: 19407024]
38. Patel SV, Erie JC, McLaren JW, Bourne WM. Keratocyte density and recovery of subbasal nerves after penetrating keratoplasty and in late endothelial failure. *Arch Ophthalmol*. 2007; 125:1693–1698. [PubMed: 18071124]
39. Al-Aqaba MA, Otri AM, Fares U, et al. Organization of the regenerated nerves in human corneal grafts. *Am J Ophthalmol*. 2012; 153:29–37.e4. [PubMed: 21907318]

40. Patel DV, Tavakoli M, Craig JP, et al. Corneal sensitivity and slit scanning in vivo confocal microscopy of the subbasal nerve plexus of the normal central and peripheral human cornea. *Cornea*. 2009; 28:735–740. [PubMed: 19574916]
41. Stachs O, Zhivov A, Kraak R, et al. Structural-functional correlations of corneal innervation after LASIK and penetrating keratoplasty. *J Refract Surg*. 2010; 26:159–167. [PubMed: 20229947]
42. Nishida T, Chikama T-I, Sawa M, et al. Differential contributions of impaired corneal sensitivity and reduced tear secretion to corneal epithelial disorders. *Jpn J Ophthalmol*. 2012; 56:20–25. [PubMed: 22071673]
43. Beuerman RW, Schimmelpfennig B. Sensory denervation of the rabbit cornea affects epithelial properties. *Exp Neurol*. 1980; 69:196–201. [PubMed: 7389846]
44. Heigle TJ, Pflugfelder SC. Aqueous tear production in patients with neurotrophic keratitis. *Cornea*. 1996; 15:135–138. [PubMed: 8925660]
45. McNamara NA, Fleiszig SM. Human tear film components bind *Pseudomonas aeruginosa*. *Adv Exp Med Biol*. 1998; 438:653–658. [PubMed: 9634950]
46. Dursun D, Monroy D, Knighton R, et al. The effects of experimental tear film removal on corneal surface regularity and barrier function. *Am J Ophthalmol*. 2000; 107:1754–1760.
47. Murphy PJ, Patel S, Marshall J. The effect of long-term, daily contact lens wear on corneal sensitivity. *Cornea*. 2001; 20:264–269. [PubMed: 11322414]
48. Patel SV, McLaren JW, Hodge DO, Bourne WM. Confocal microscopy in vivo in corneas of long-term contact lens wearers. *Invest Ophthalmol Vis Sci*. 2002; 43:995–1003. [PubMed: 11923239]
49. Oliveira-Soto L, Efron N. Morphology of corneal nerves in soft contact lens wear. A comparative study using confocal microscopy. *Ophthalmic Physiol Opt*. 2003; 23:163–174. [PubMed: 12641704]
50. Azari AA, Rapuano CJ. Autologous Serum Eye Drops for the Treatment of Ocular Surface Disease. *Eye Contact Lens*. 2015
51. Tsubota K, Goto E, Shimmura S, Shimazaki J. Treatment of persistent corneal epithelial defect by autologous serum application. *Am J Ophthalmol*. 1999; 106:1984–1989.
52. Pushker N, Dada T, Vajpayee RB, et al. Neurotrophic keratopathy. *CLAO J*. 2001; 27:100–107. [PubMed: 11352446]

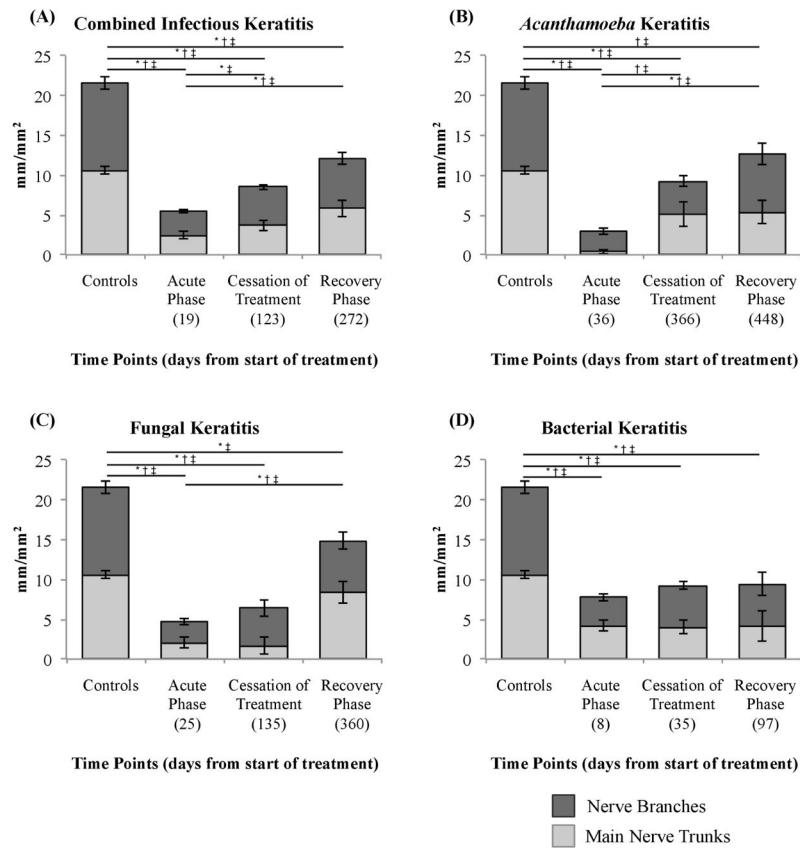


**Figure 1.**

(A) *In vivo* confocal microscopy image of normal corneal subbasal nerve plexus in a normal control group. (B) All nerves were traced using Neuron J, including the main nerve trunks (red tracings) and nerve branches (green tracings).

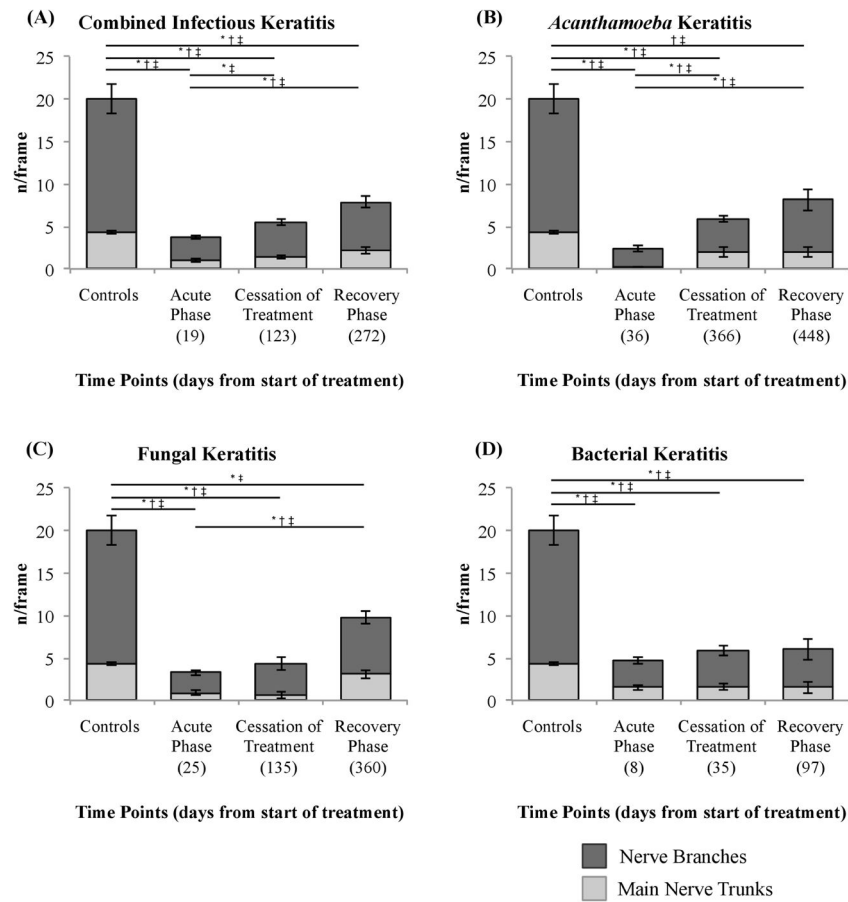


**Figure 2.** Slit-lamp photographs and *in vivo* confocal microscopy (IVCM) images obtained at the level of the corneal subbasal nerve plexus. **(A–C)** IVCM of *Acanthamoeba* keratitis during the acute phase **(A)**, cessation of the treatment **(B)** and recovery phase **(C)**. **(D–F)** IVCM of fungal keratitis during the acute phase **(D)**, cessation of treatment **(E)** and recovery phase **(F)**. **(G–I)** IVCM of bacterial keratitis during the acute phase **(G)**, cessation of treatment **(H)** and recovery phase **(I)**.

**Figure 3.**

Bar graphs showing subbasal corneal nerve length alterations in infectious keratitis and controls during the acute phase, cessation of treatment, and recovery phase. **(A)** Infectious keratitis combined, **(B)** *Acanthamoeba* keratitis, **(C)** fungal keratitis and **(D)** bacterial keratitis. Bars indicate mean  $\pm$  standard error of the mean. \* =  $p < 0.05$  for nerve branches, † =  $p < 0.05$  for main nerve trunks and ‡ =  $p < 0.05$  for total of nerves.



**Figure 4.**

Bar graphs showing subbasal corneal nerve number alterations in controls and infectious keratitis groups during the acute phase, cessation of treatment, and recovery phase. **(A)** Infectious keratitis combined, **(B)** *Acanthamoeba* keratitis, **(C)** fungal keratitis and **(D)** bacterial keratitis. Bars indicate mean  $\pm$  standard error of the mean. \* =  $p < 0.05$  for nerve branches, † =  $p < 0.05$  for main nerve trunks and ‡ =  $p < 0.05$  for total of nerves.

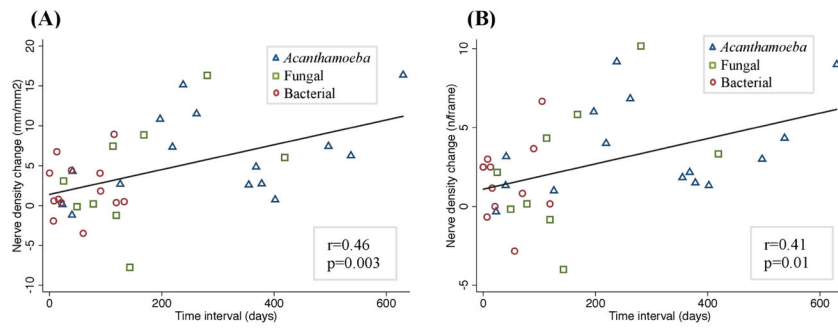


**Figure 5.**

Scatter plot showing the correlation between the subbasal corneal nerve alterations over time. A significant positive correlation was found between the changes in total nerve length (A) and total number of nerve (B) with the time interval between the time points. Spearman's correlation coefficient was used.

**Table 1**  
Demographics and treatment duration in patients with infectious keratitis and normal controls.

	Controls	Infectious Keratitis Combined	<i>Acanthamoeba</i> Keratitis	Fungal Keratitis	Bacterial Keratitis
Eyes, n	30	56	13	15	28
Sex, n (Male/Female)	10/20	31/25	8/5	7/8	16/12
Age, (yrs)	42.3 ± 2.1	42.4 ± 2.1	35.7 ± 3.4	51.9 ± 2.7	40.8 ± 3.4
Contact lens use, n (%)	18 (60)	42 (75)	13 (100)	10 (66)	20 (71)
Duration of treatment (days)	—	123.5 ± 26.8	366.8 ± 73.4	135.4 ± 31.8	35.3 ± 5.7

**Table 2**

Corneal subbasal nerve parameters in controls and infectious keratitis patients.

	Controls	Combined Infectious Keratitis		
		Acute Phase	Cessation of Treatment	Recovery Phase
Total nerve length, mm/mm <sup>2</sup>	21.59 ± 1.06	5.47 ± 0.69*	8.49 ± 0.94*†	12.13 ± 1.97*†
Main nerve trunk length, mm/mm <sup>2</sup>	10.61 ± 0.46	2.44 ± 0.42*	3.69 ± 0.64*	5.80 ± 1.00*†
Nerve branch length, mm/mm <sup>2</sup>	10.98 ± 0.80	3.03 ± 0.24*	4.80 ± 0.37*†	6.33 ± 0.76*†
Total nerve number, n/frame	20.00 ± 1.80	3.70 ± 0.35*	5.50 ± 0.55*†	7.85 ± 1.16*†
Main nerve trunk number, n/frame	4.35 ± 0.19	0.99 ± 0.17*	1.43 ± 0.25*	2.14 ± 0.36*†
Nerve branch number, n/frame	15.65 ± 1.65	2.71 ± 0.20*	4.07 ± 0.34*†	5.71 ± 0.66*†

Values are reported as mean ± standard error of the mean.

\* Statistical significance (p<0.05) compared to controls.

† Statistical significance (p<0.05) compared to acute phase.

Table 3

Corneal subbasal nerve parameters in infectious keratitis subgroups.

	<i>Acanthamoeba</i> Keratitis			Fungal Keratitis			Bacteria Keratitis		
	Acute Phase	Cessation of Treatment	Recovery Phase	Acute Phase	Cessation of Treatment	Recovery Phase	Acute Phase	Cessation of Treatment	Recovery Phase
Total nerve length, mm/m <sup>2</sup>	2.91 ± 0.64*	9.24 ± 1.97* <sup>†</sup>	12.70 ± 2.77* <sup>†</sup>	4.65 ± 0.95*	6.37 ± 2.00*	14.85 ± 3.12 <sup>†</sup>	7.71 ± 1.24*	9.18 ± 1.81*	9.39 ± 3.28*
Main nerve trunk length, mm/m <sup>2</sup>	0.37 ± 0.24*	5.09 ± 1.51* <sup>†</sup>	5.38 ± 1.50* <sup>†</sup>	2.07 ± 0.67*	1.62 ± 1.06*	8.38 ± 1.43 <sup>†</sup>	4.16 ± 0.70*	4.02 ± 0.82*	4.16 ± 1.91*
Nerve branch length, mm/m <sup>2</sup>	2.54 ± 0.42*	4.15 ± 0.63*	7.32 ± 1.36 <sup>†</sup>	2.58 ± 0.35*	4.75 ± 0.99*	6.47 ± 1.04 <sup>†</sup>	3.55 ± 0.40*	5.16 ± 0.49*	5.23 ± 1.48*
Total nerve number, n/frame	2.36 ± 0.40*	5.91 ± 0.87* <sup>†</sup>	8.12 ± 1.77* <sup>†</sup>	3.27 ± 0.53*	4.38 ± 1.16*	9.82 ± 2.26 <sup>†</sup>	4.66 ± 0.65*	5.85 ± 1.02*	5.99 ± 2.16*
Main nerve trunk number, n/frame	0.15 ± 0.10*	1.97 ± 0.60* <sup>†</sup>	1.96 ± 0.56* <sup>†</sup>	0.85 ± 0.29*	0.58 ± 0.38*	3.08 ± 0.47 <sup>†</sup>	1.52 ± 0.29*	1.58 ± 0.33*	1.56 ± 0.70*
Nerve branch number, n/frame	2.21 ± 0.32*	3.94 ± 0.36* <sup>†</sup>	6.16 ± 1.24 <sup>†</sup>	2.42 ± 0.31*	3.80 ± 0.79*	6.74 ± 0.78 <sup>†</sup>	3.14 ± 0.35*	4.27 ± 0.56*	4.43 ± 1.20*

Values are reported as mean ± standard error of the mean.

\* Statistical significance (p<0.05) compared to controls.

<sup>†</sup> Statistical significance (p<0.05) compared to acute phase.